Validation of GNSS orbits using SLR observations

Claudia Urschl[1], Gerhard Beutler[1], Werner Gurtner[1], Urs Hugentobler[1], Stefan Schaer[2]

[1] *Astronomical Institute, University of Bern, Switzerland*
[2] *Federal Office of Topography, swisstopo, Wabern, Switzerland*

Abstract

Precise GNSS orbits at the centimeter level are routinely generated by the IGS analysis centers using microwave phase measurements. For those GNSS satellites equipped with retroreflector arrays SLR observations are available. They are very useful for validating the microwave-based GNSS orbits. We present recent SLR validation results of GPS and GLONASS orbits derived from microwave phase observations. Four years (2002-2005) of SLR range residuals have been analyzed. Inter-technique biases of several centimeters could be confirmed. Periodic variations of the range residuals with maxima at the eclipse seasons indicate orbit modeling deficiencies for the GPS satellites. The results clearly demonstrate the need for retroreflector arrays for each GNSS satellite type for an independent validation of the microwave measurement technique.

1 Introduction

SLR (Satellite Laser Ranging) observations allow for a completely independent validation of microwave-based GNSS (Global Navigation Satellite Systems, at present consisting of GPS and GLONASS) orbits. On the other hand, SLR tracking data may be validated as well. All GLONASS satellites but only two of the currently active 29 GPS satellites are equipped with Laser retroreflector arrays (LRA). Both GPS satellites, PRN G05 and G06, and a subset of three GLONASS satellites are routinely tracked by the SLR community. Several analyses in the past have shown systematic biases between the microwave-based GPS orbits and the SLR observations, as well as periodic patterns in the SLR range residuals (see, e.g., Appleby and Otsubo, 2000; Springer, 2000; Urschl et al., 2005). Until now it was, however, not clear whether these systematic effects could be assigned to orbit modeling deficiencies or to SLR tracking biases. Subsequently, we present new SLR validation results, which clearly point to serious GPS orbit modeling problems.

2 Validation method

The validation process is based on the analysis of SLR range residuals, the differences between the observed Laser ranges and the ranges computed from the orbital information relying on microwave phase data. SLR measurements of the last 4 years were used starting in 2002 for the two GPS satellites and four GLONASS satellites. Table 1 lists the satellite numbers and the corresponding retroreflector offsets, i.e., the difference vectors between the LRA center of reflection and the satellite's center of mass, which have been added to the Laser range for the computation of the range

Satellite type	No.	PRN Code	COSPAR-ID	$x(m)$	$y(m)$	$z(m)$
GPS	35	G05	1993-054A	0.8626	-0.5245	0.6695
GPS	36	G06	1994-016A	0.8626	-0.5245	0.6717
GLONASS	87	R03	2001-053B	0.0000	0.0000	1.5416
GLONASS	89	R22	2002-060A	0.0000	0.0000	1.5416
GLONASS	84	R24	2000-063B	0.0000	0.0000	1.5416
GLONASS-M	95	R07	2004-053B	0.1370	0.0000	1.9010

Table 1: Laser retroreflector offsets used for GPS and GLONASS satellites in the satellite's body-fixed coordinate system. (Note that the offsets have been updated recently, details are given in Section 2.)

residuals. The reflector offsets are given in the satellite's body-fixed coordinate system, a right hand system with the origin at the center of mass, the x-axis positive towards the hemisphere that contains the Sun, the y-axis pointing along the solar panel axis perpendicular to the Sun-satellite vector, and the z-axis pointing to the center of the Earth. In November 2005, the GLONASS satellite R24 was replaced in the SLR tracking scheme by R07, one of the new GLONASS-M satellites. The z-offset for the GPS satellites was corrected by about $1\,cm$ due to a tray segment between the LRA and the spacecraft not considered before (Davis et al., 2005). According to most recent information provided by the International Laser Ranging Service (ILRS, 2006), the retroreflector offsets for the newer GLONASS satellites are now confirmed and differ at the cm-level mainly in z-direction from the values used in our analysis. The correct values in meters are (0, 0, 1.555) for the GLONASS satellites R03, R22, R24 and (0.137, 0.003, 1.874) for the GLONASS-M satellite R07.

The SLR data used are so-called normal points, which are formed by averaging the individual range measurements over a certain time interval (5 min for GNSS satellites). Normal points based on a very small number of data points (i.e., less than 12 data points) have been excluded from our analysis.

SLR measurements to eclipsing GPS satellites are treated separately, because of the particular rotational behavior of BLOCK IIA satellites during eclipse: When the satellite enters the Earth's shadow, it starts rotating around its z-axis (pointing to the geocenter) with maximum rate. The maximum rotation rate of the solar panel axis (y-axis) around the z-axis is about $0.12\,°/sec$ (Bar-Sever, 1994). After shadow exit, the satellite may need another 30 minutes to reach its nominal attitude. As opposed to the GLONASS satellites, the LRA is not centered on the z-axis, which results in biased range measurements during the eclipse phase, if the rotation rate is not modeled correctly. Therefore, we apply the rotation rates provided by JPL for eclipsing GPS satellites. Figure 1 shows the range residuals during the eclipse phases for PRN G06 without (left) and with (right) applying the yaw rotation rates. Range residuals outside eclipse are marked in blue, whereas residuals from observations during eclipse are marked in orange. The range residuals can be improved significantly by modeling the satellite's attitude correctly within the Earth's shadow.

Several microwave-based orbits have been validated: the CODE final and rapid product, GFZ final orbits, JPL final orbits, as well as the combined IGS final orbits. The Bernese GPS Software V5.0 (Hugentobler et al., 2005) was used for all tests. The time series for the CODE final orbits was treated in two parts because a model change took place in November 2005, when the a priori solar radiation pressure model ROCK was replaced by the CODE solar radiation pressure model. In addition, a wrong sign for the general relativistic correction of the force model was corrected, which reduced the orbit scale by about $0.4\,ppb$.

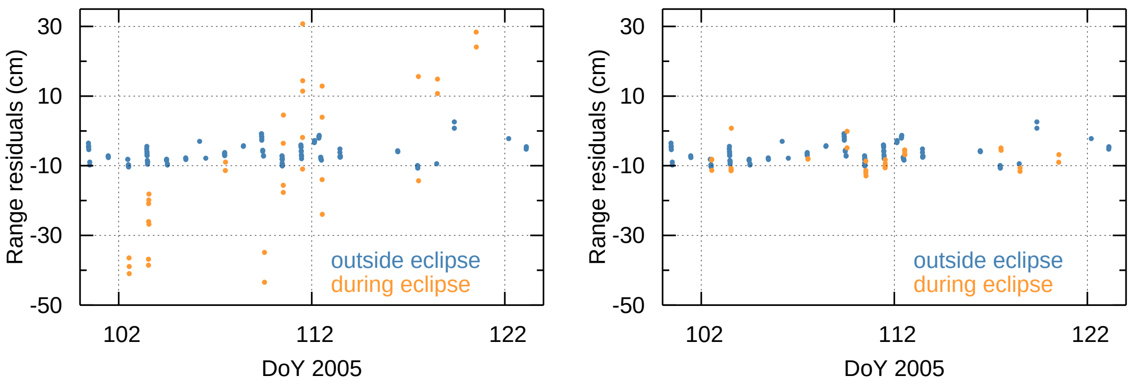

Figure 1: SLR range residuals derived from CODE final orbits for the GPS satellite PRN G06, outside and during eclipse; **left:** without applying yaw rotation rates, **right:** with applying yaw rotation rates.

3 Validation results

Figures 2(a) and 2(b) show the range residuals derived from the CODE final orbits for the two GPS satellites PRN G05 and G06. Figure 3 shows the residuals for the GLONASS satellites PRN R03, R22, R24 and the GLONASS-M satellite R07. The residuals are drawn as a function of time. The different colors indicate the different orbit models used for the CODE final orbit (black - before the model change, blue - after the model change). A mean bias of about $-4\,cm$ can be observed. The negative sign indicates that the distance to the satellite measured with SLR is shorter than the distance derived from the microwave-based orbits. The standard deviation is about $2-3\,cm$. This value stands primarily for the radial accuracy of the three-day arcs. The statistical information of the solutions performed is summarized in Table 2. It gives the standard deviation and the associated range biases in cm for all final orbit products considered. The last two columns give the number of normal points. In addition to the CODE final orbit, SLR validation results of the GFZ, JPL, and IGS final GPS orbits are included. Values corresponding to the CODE final orbit after the model change are given in blue color.

The standard deviation (i.e., the root mean square deviation from the arithmetic mean) of the range residuals for the GPS orbits is about $2-3\,cm$. The range bias (i.e., the arithmetic mean) differs by up to $1\,cm$ between the orbit solutions, reflecting the orbital scale differences. For the CODE orbits

Sat	Standard deviation (cm)					Range bias (cm)					Number of
	COD	COD	GFZ	JPL	IGS	COD	COD	GFZ	JPL	IGS	normal points
G05	2.2	1.8	2.3	2.2	1.9	-4.4	-3.5	-3.6	-2.6	-3.1	10100 (1300)
G06	2.7	2.2	2.7	2.5	2.5	-4.8	-3.2	-3.9	-2.8	-2.8	9800 (1100)
R03	4.7	5.6				-3.3	-1.5				14800 (2800)
R22	4.4	5.1				-2.7	-1.3				18500 (2500)
R24	5.1					-2.6					12600
R07	4.6	5.8				1.4	3.6				1500 (1700)

Table 2: Statistical information for the SLR range residuals derived from microwave-based GNSS orbits: standard deviation (cm), range bias (cm), and number of normal points.

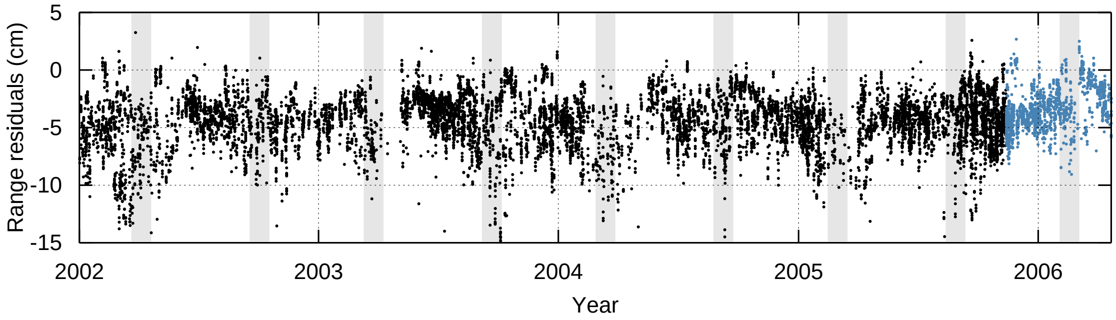

(a) PRN G05

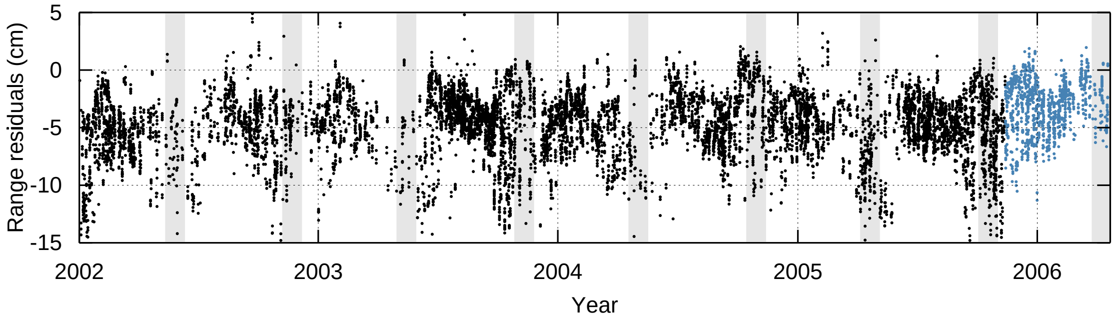

(b) PRN G06

Figure 2: SLR range residuals derived from CODE final orbits for the GPS satellites PRN G05 and G06; the shaded areas indicate eclipse seasons.

the scale was reduced by about $0.4\,ppb$ ($1\,cm$) after the model change in November 2005. The new retroreflector offset in z-direction decreases the range bias by $1\,cm$. With these recent improvements the mean bias for GPS satellites is now between $-3\,cm$ and $-4\,cm$. A standard deviation of $5\,cm$ results for the GLONASS satellites. The lower orbit quality compared to GPS is mainly due to the much sparse IGS network tracking GLONASS satellites. The mean range bias for the GLONASS satellite type is at $-1.5\,cm$ after the model change, whereas for the new GLONASS-M satellite type a positive bias of $3.6\,cm$ is estimated. The retroreflector offsets used (see Table 1) have not been confirmed at the time of our analysis. The new official values (ILRS, 2006) differ, however, from our values used. Thus, the z-component of the retroreflector offsets change for the GLONASS satellites by $1.34\,cm$ and for GLONASS-M by $-2.7\,cm$, which does nearly compensate the estimated biases.

For each of the GPS orbits, we observe a periodic pattern with residuals of up to $10\,cm$ amplitude, systematically pointing into one direction. The largest residuals occur at eclipse seasons, when the satellite is observed within the Earth shadow (indicated with shaded areas in Figures 2(a) and 2(b)). But those systematically large residuals are not only restricted to the shadow periods. Since both, observation geometry as well as orbit-Sun geometry repeat with the same period of about 351 days (the repeat period of the Sun with respect to the satellite constellation that may be called the “draconitic GPS year” referring to the regressive nodes of the orbital planes), it is not possible to assign the source of the periodic pattern to the SLR or to the microwave observation technique.

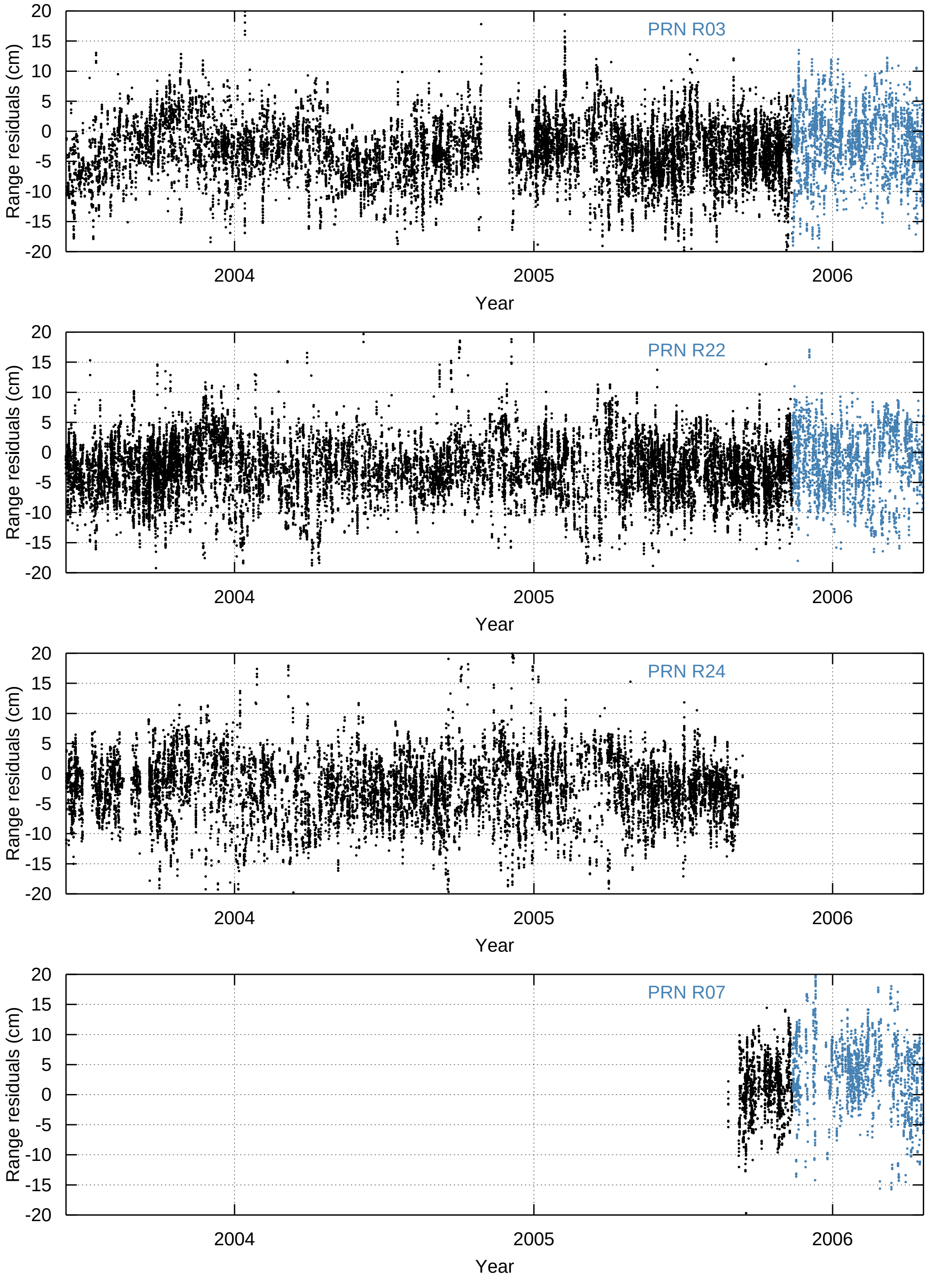

Figure 3: SLR range residuals derived from CODE final orbits for the GLONASS satellites PRN R03, R22, R24, and the GLONASS-M satellite R07.

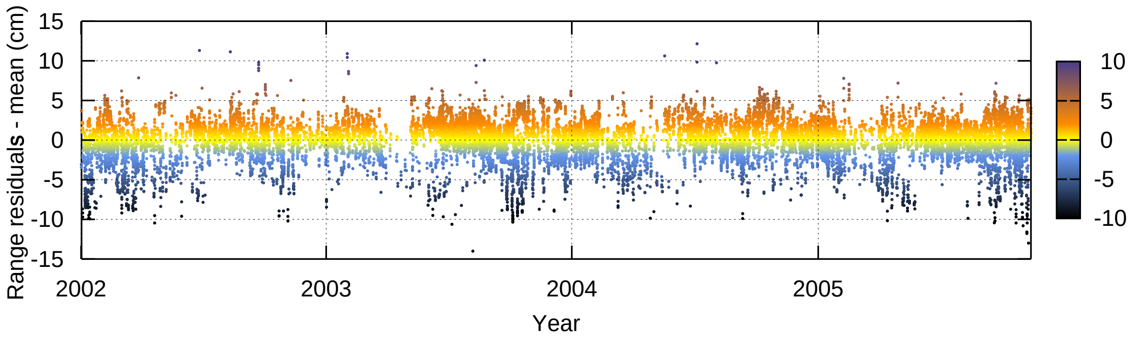

Figure 4: Color-coded SLR range residuals (cm) minus mean value derived from CODE final orbits for the GPS satellites PRN G05 and G06.

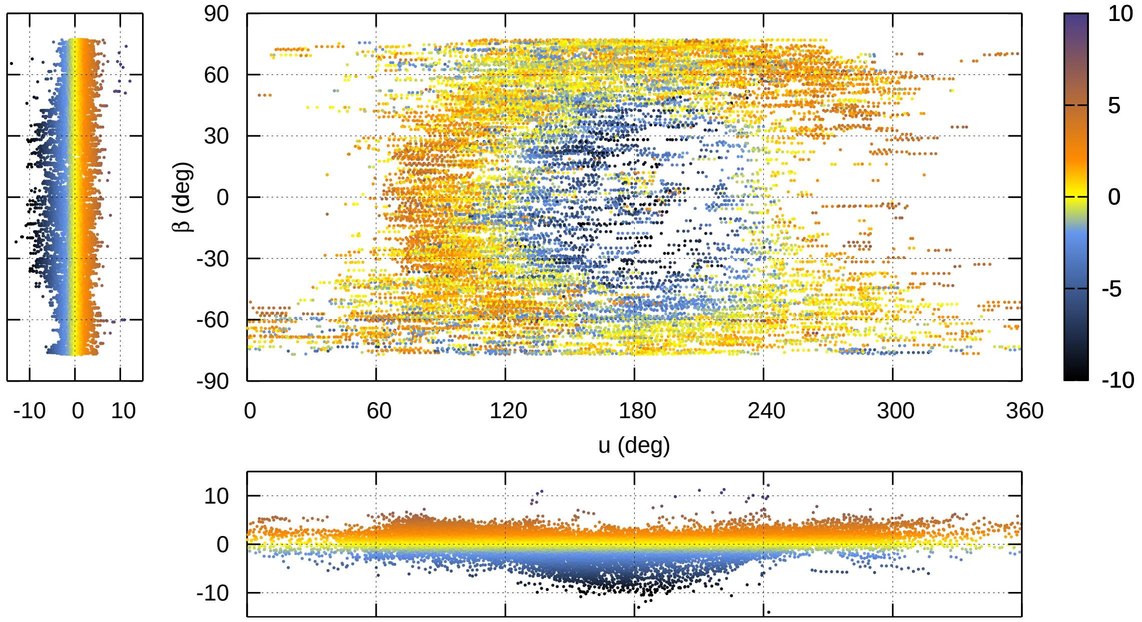

Figure 5: Color-coded SLR range residuals (cm) minus mean value derived from CODE final orbits for the GPS satellites PRN G05 and G06 in the (u, β)-coordinate system; **left:** projection to β-axis, **bottom:** projection to u-axis.

Therefore, the following experiment was performed. Because the residuals for both GPS satellites show the same pattern, we analyze them together. We subtract the mean bias from the range residuals and color the resulting residuals depending on their values as displayed in Figure 4. These colored range residuals are now displayed in the (u, β)-coordinate system, where β is the elevation of the Sun above the satellite's orbital plane and u is the argument of latitude of the satellite with respect to the argument of latitude of the Sun. Figure 5 shows the color-coded range residuals for both GPS satellites derived from the CODE final orbits in this system. Thus the residuals are projected to the celestial sphere with the Earth's shadow at the center of the figure.

In the course of its orbital revolution a satellite crosses the figure from left to right. If $\beta = 0°$, the Sun lies in the orbital plane and if, in addition, $u = 180°$ the satellite is in the deepest shadow. At the opposite side of the orbital plane ($u = 0°$), no SLR observations are available, because the satellite is very close to the Sun for all Laser measurements. We observe a systematic pattern with the largest values for shadow passes, but large systematic effects are not restricted to the shadow passes. The two small subfigures at the left and the bottom of the (u, β)-figure show the projections of the

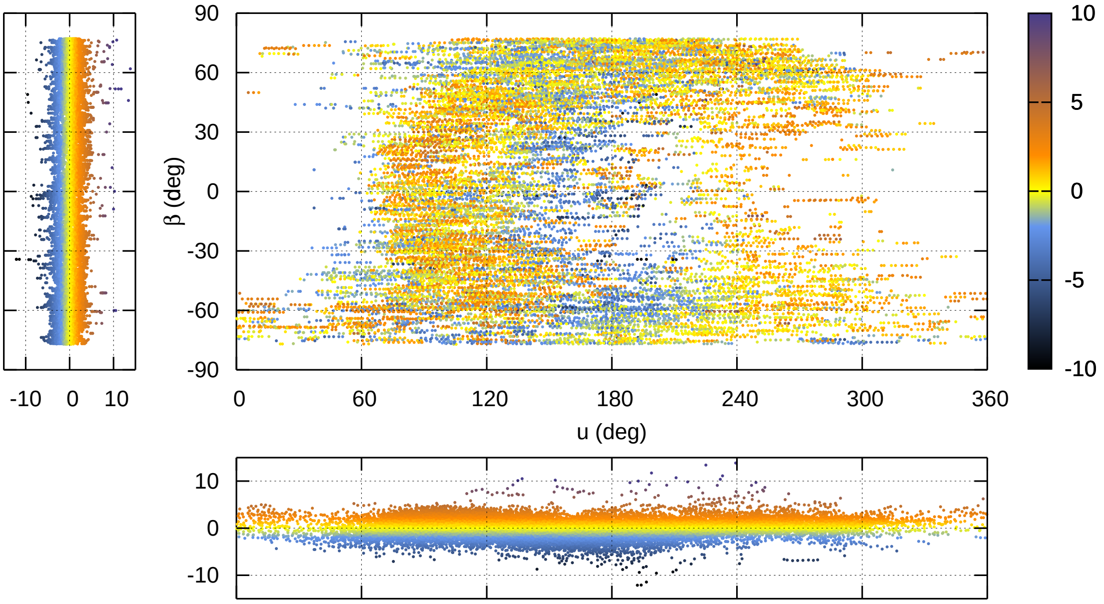

Figure 6: Color-coded SLR range residuals (cm) minus mean value derived from CODE rapid orbits for the GPS satellites PRN G05 and G06 in the (u, β)-coordinate system; **left:** projection to β-axis, **bottom:** projection to u-axis.

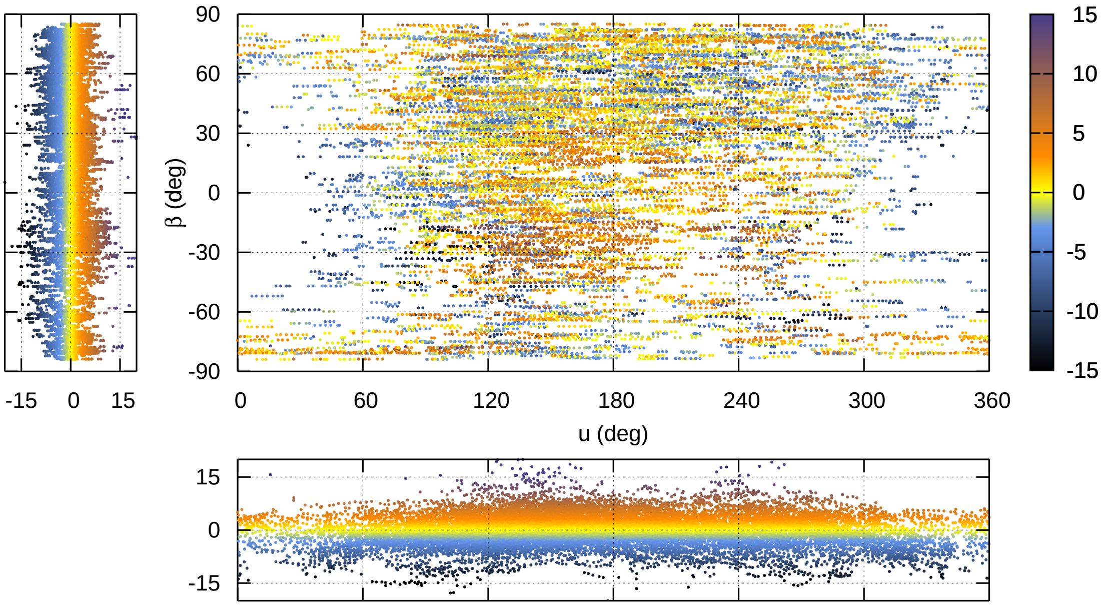

Figure 7: Color-coded SLR range residuals (cm) minus mean value derived from CODE final orbits for the GLONASS satellite PRN R22 in the (u, β)-coordinate system; **left:** projection to β-axis, **bottom:** projection to u-axis.

residuals onto the β- and u-axis, respectively. The dependency of the residuals on the satellite's position within the orbital plane is clearly visible. The IGS, GFZ as well as the JPL microwave-based orbits show similar patterns. The pattern does not depend on the SLR stations. If the range residuals are considered station by station, the same signature is observed.

Figure 6 shows the range residuals for both GPS satellites derived from the CODE rapid orbits. Although there is still a systematic pattern, it is less pronounced and the largest residuals of $-10\,cm$ disappeared. The explanation for the difference of results based on CODE rapid and final orbits, respectively, are most likely due to the a priori solar radiation pressure models used. For the generation of the rapid orbit product the CODE radiation pressure model was used (Springer et al., 1999), whereas for the final product the ROCK model (Fliegel et al., 1992) was still used before the model change in November 2005. Figure 7 shows the color-coded range residuals for one of the GLONASS satellites (PRN R22) derived from the CODE final orbits. We do not see a systematic pattern for any of the GLONASS satellites, but rather randomly distributed (although larger) residuals. It is interesting to note that no a priori radiation pressure model was used for the generation of the CODE GLONASS orbits till now.

4 Summary

From our experiments we draw the following conclusions: The periodic signature in the range residuals of the GPS satellites is not caused by the SLR tracking data, but due to the GNSS analysis. The systematic behavior of the SLR residuals is most likely due to deficiencies in the orbit model. Currently, we believe that an improved radiation pressure model, based on an analysis of the recent ten years of GPS orbits might cure the problem. Earth albedo radiation pressure was not yet considered in the orbit modeling, but it might have a non-negligible effect on the orbit. Attitude modeling problems as, e.g., a misorientation of the z-axis may cause a similar pattern of the residuals, but to explain amplitudes of up to $10\,cm$ an Earth pointing error of up to 6° would be necessary, which probably rules out this explanation.

SLR observations prove to be extremely useful for an independent validation of microwave-based GNSS orbits. Although the GPS orbits of the individual IGS analysis centers are consistent at the $2\,cm$ level, systematic range residuals of up to $10\,cm$ reveal orbit or attitude modeling deficiencies. Further studies are needed to understand the source of the inter-technique biases and the periodic pattern of the range residuals. The inconsistencies between different observation techniques demonstrate the need for co-location of measurement types at the satellites. SLR retroreflectors should not be considered as a luxuries for new GNSS satellites. At least one reflector array for each satellite type (and orbital plane) is a necessity.

Acknowledgment

This work is supported by the Swiss National Science Foundation (SNF). Data used in this study was provided by the ILRS (Gurtner et al., 2002) and the IGS (Beutler et al., 1999).

References

Appleby G, Otsubo T (2000) Comparison of SLR measurements and orbits with GLONASS and GPS microwave orbits. In: Proc. of 12th International Workshop on Laser Ranging, Matera, Italy, November 13-17

Bar-Sever J (1994) Improvement to the GPS attitude control subsystem enables predictable attitude during eclipse seasons. IGS Mail #0591, May 1994

Beutler G, Rothacher M, Schaer S, Springer TA, Kouba J, Neilan RE (1999) The International GPS Service (IGS): An interdisciplinary service in support of Earth sciences. Adv Space Res 23(4): 631-635

Davis M, Trask A, Middour J, Hope A, Moore C, Scharpf W, Smith R, Suite M, Burris H, Stella M (2005) NGA GPS Navigation accuracy assessment using SLR techniques. Unpublished manuscript, March 2005

Fliegel HF, Gallini TE, Swift ER (1992) Global positioning system radiation force model for geodetic applications. J Geophys Res 97(B1): 559-568

Gurtner W, Noomen R, Pearlman MR (2004) The International Laser Ranging Service: current status and future developments. Adv Space Res 36: 327-332

Hugentobler U, Schaer S, Fridez P (2005) Bernese GPS Software Version 5.0. Druckerei der Universität Bern, Switzerland

ILRS (2006) SLR Satellite Center-of-Mass Offset Information. Available at http://ilrs.gsfc.nasa.gov/satellite_missions/center_of_mass/index.html, May 2006

Springer TA, Beutler G, Rothacher M (1999) A new solar radiation pressure model for GPS. Adv Space Res 23(4): 673-676

Springer TA (2000) Modeling and validating orbits and clocks using the Global Positioning System. Geodätisch-geophysikalische Arbeiten in der Schweiz 60, Schweizerische Geodätische Kommission

Urschl C, Gurtner W, Hugentobler U, Schaer S, Beutler G (2005) Validation of GNSS orbits using SLR observations. Adv Space Res 36(3): 412-417